BNL-45182
CONF-8909178--2

Invited Paper for the U.S.-Korea Joint Seminar on Fluids Engineering and Science, Seoul, Korea, September 3–9, 1989.

BNL--45182

DE91 001129

PHASE PORTRAIT METHODS FOR VERIFYING FLUID DYNAMIC SIMULATIONS

H. Bruce Stewart

Mathematical Sciences Division

Department of Applied Science

Brookhaven National Laboratory

Upton, New York 11973

This work was supported by the Applied Mathematical Sciences program of the U.S. Department of Energy under Contract No. DE-AC02-76CH00016.

INTRODUCTION

As computing resources become more powerful and accessible, engineers more frequently face the difficult and challenging engineering problem of accurately simulating nonlinear dynamic phenomena. Although mathematical models are usually available, in the form of initial value problems for differential equations, the behavior of the solutions of nonlinear models is often poorly understood. A notable example is fluid dynamics: while the Navier-Stokes equations are believed to correctly describe turbulent flow, no exact mathematical solution of these equations in the turbulent regime is known. Differential equations can of course be solved numerically, but how are we to assess numerical solutions of complex phenomena without some understanding of the mathematical problem and its solutions to guide us?

DYNAMICAL SYSTEMS AND RECURRENCE

One of the few approaches to dynamics applicable to general nonlinear problems is the qualitative, geometric theory initiated by Poincaré. Nonlinear dynamic phenomena may be informally divided into two classes, rapid transients and recurrent behavior; qualitative dynamics has much to say about the latter. The word dynamics is used here to stand for the more long-winded description *dynamical systems theory*, since we are dealing not with a restricted branch of mechanics, but with any system whose evolution is described mathematically as an initial value problem. The qualitative theory describes phenomena which behave essentially as a closed system under at most a few, well-known external influences; this means that any explicitly time-dependent terms, or forcing functions, in the differential equations are few and simple. In many cases the mathematical model of the time evolution is an *autonomous* system of equations with no explicit time dependence — the system is presumed to run like a complex but deterministic clockwork. Examples would be the Navier-Stokes equations for fluid flow in a pipe with constant inflow conditions; or the Oberbeck-Boussinesq equations for thermal correction in a rectangular cavity heated from below and cooled above at a constant rate.

Recurrent behavior in a dynamical system can occur after start up transients have decayed, and is identified by the property that given any post-transient state of the system, the dynamics will return the system arbitrarily close to that state after a sufficient time. The simplest recurrent behavior types are *equilibrium* (the system returns to equilibrium state by never leaving it) and *periodic motion* (the system returns exactly after a fixed time, the period of the motion). Nonperiodic recurrence occurs in the motion of the solar system; because the planets have different periods and their periods are not related as ratios of integers, the solar system as a whole never returns precisely to the same state; but recurrence is evidenced for example by eclipses which occur at irregular but predictable intervals.

Examples of recurrent dynamic behavior in fluid engineering include chattering of valves, flow induced structural vibrations, and parallel channel flow instabilities. These and many other practical problems are amenable to qualitative study as nonlinear dynamical systems.

CHAOTIC DYNAMICS AND CHAOTIC ATTRACTORS

A recent discovery of qualitative dynamical systems theory of concern to all engineers is the discovery of chaotic recurrent behavior in many simple nonlinear dynamical systems. Here *chaos* is a technical term, recently coined to describe simple deterministic systems (e.g. initial value problems for ordinary differential equations) which nevertheless behave in a way which is in some aspect completely random. In fact this seeming paradox of random behavior in a deterministic system is not only possible, but typical and common in nonlinear dynamical systems. This discovery is of obvious concern to engineers, implying to the pessimist that even simple dynamical systems may behave unpredictably; while to the optimist it suggests that apparently random behavior may have a very simple explanation.

Let us consider a specific equation, the periodically forced Duffing oscillator

$$\ddot{x} + 0.05\dot{x} + x^3 = 7.5\cos t.$$

This equation describes the mechanical vibration of a vertically loaded support column under time-periodic lateral forcing; it has been studied extensively by Ueda[**1**]. Note that we have chosen specific numerical coefficients, but these are not special values; similar behavior occurs for a substantial range of values, as suggested by Figure 1. Figure 2 shows a typical steady state chaotic history of a solution $x(t)$ versus time, after initial transients have decayed. The behavior is recurrent but not periodic. Superimposed on Figure 2 is a second solution started very close to the first; the two solutions diverge rapidly and soon become uncorrelated. This divergence from nearly identical starting conditions is the cause of long-term unpredictability of this chaotic behavior.

The key to understanding this behavior is the qualitative geometric dynamics introduced by Poincaré. His geometry is the geometry of phase space, the abstract space whose coordinates are all the state variables of a dynamical system. The Duffing equation gives the acceleration in terms of x, $\dot{x}$, and t, and we must examine trajectories traced out in the three-dimensional $(x, \dot{x}, t)$ phase space by integrating the differential equation. Furthermore, we must examine the geometry not of one solution curve, but of a large number representing all solutions.

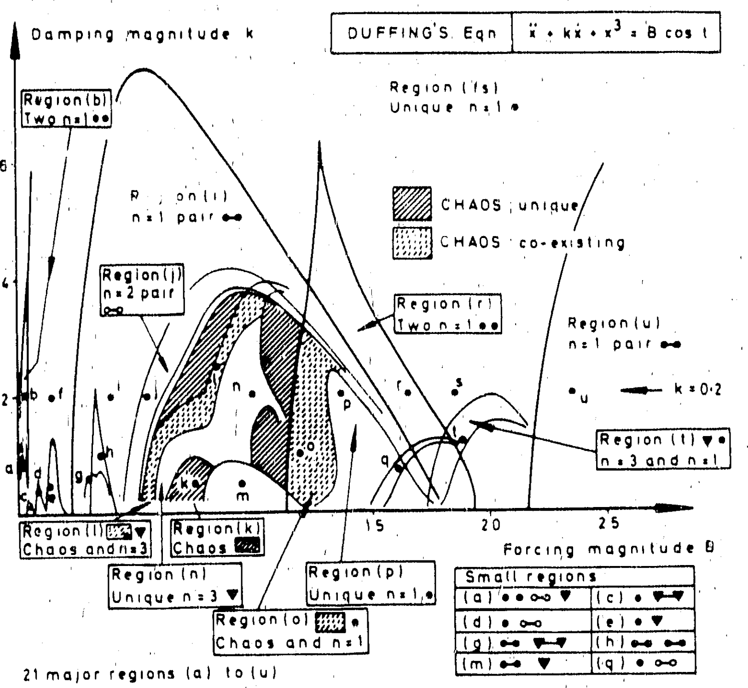

FIGURE 1. Regions of subharmonic and chaotic response of Duffing's equation (from ref. 3, after Ueda, ref. 1)

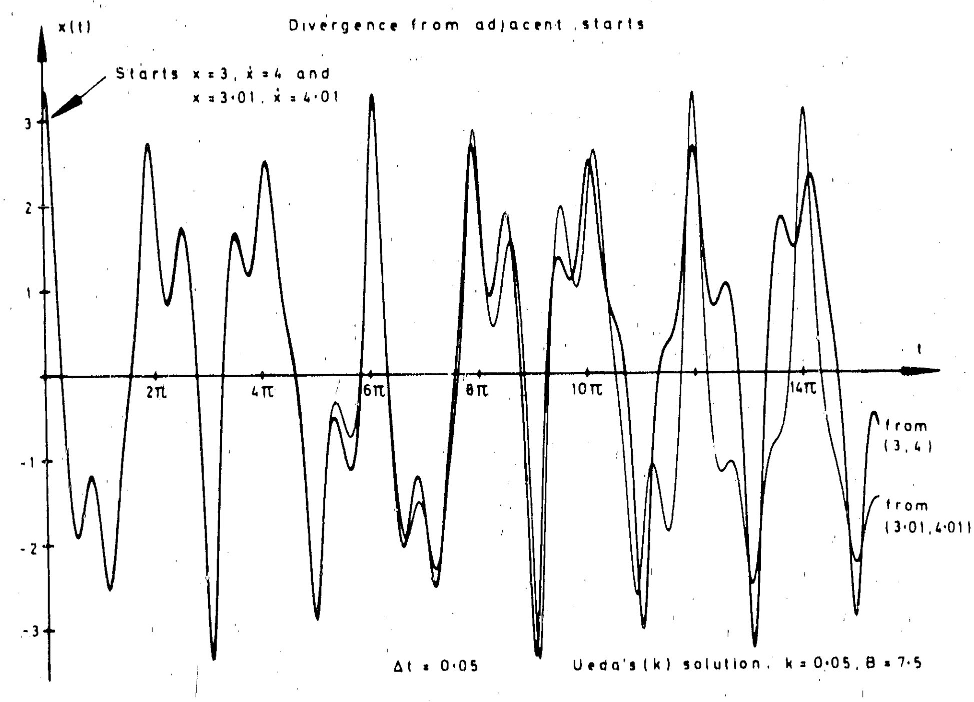

FIGURE 2. Chaotic oscillations in Duffing's equation (from ref. 3)

Following all solutions of this or any typical dissipative dynamical system to their final long-term behavior, we find that curves which initially fill the phase space eventually settle down to motion in a small subregion called the *attractor*. If the final behavior is equilibrium, the attractor is a stable *fixed point* in phase space whose coordinates identify the equilibrium state. If the final behavior is periodic, all solutions settle onto a simple closed loop in phase space, a *limit cycle*. In chaotic behavior, there is also a well-defined structure to which transient curves settle; this is the *chaotic attractor*. A glimpse of this structure is shown in Figure 3 using a mathematical device known as the Poincaré section, which shows the location in the $(x, \dot{x})$ plane of a bundle of post-transient trajectories frozen at one instant in time. In this case, the dots may be thought of as the stroboscopic images of a single trajectory sampled only at discrete times $t = 0, 2\pi, 4\pi, \ldots$ when the periodic forcing is at angle zero. As time progresses, dots would appear to fall haphazardly; only with the accumulation of many recurrences does the structure of this chaotic attractor become evident. The phase space geometry of nonlinear dynamical systems and chaotic dynamics is described more fully in references 2 and 3.

DIMENSION OF CHAOTIC ATTRACTORS

Phase space portraits can be helpful in understanding many kinds of nonlinear oscillation. Phase space is an abstract space, and qualitative geometric methods were used mainly by mathematicians until recently, when computer graphics devices have made phase space accessible to the non-specialist. Computer simulations can be conveniently used to produce pictures of two- and three-dimensional phase space trajectories. In fact, the best way to understand chaotic attractors is to program integration of simple ordinary differential equations like the Duffing equation on a small interactive computer or workstation with a graphic display, and treat the simulation as a numerical experiment.

The limitation on the geometric approach would seem to be the difficulty of visualizing higher dimensional space. Engineers used to dealing with mathematical models based on hundreds or thousands of unknown state variables may wonder whether the geometry of an abstract space with as many dimensions can lead to any understanding.

In fact, even large dynamical systems can settle into chaotic steady state behavior in a subset of phase space confined to three dimensions. Figure 4 shows one example, from a numerical simulation of a confined air-water jet using a two-dimensional model with about 400 unknowns per time step; examination of this orbit using interactive computer graphics has confirmed that it is entirely consistent with a vector field in a three-dimensioned phase space. The physical cause of this is *dis-*

FIGURE 3. Poincaré section in the $(x, \dot{x} = y)$ plane showing 100,000 points of a trajectory settled onto the chaotic attractor of Duffing's equation with $k = 0.05, B = 7.5$ (courtesy of Y. Ueda)

sipation, in the form of friction, heat conduction, viscosity, and so on. Liouville's theorem on energy-conserving Hamiltonian systems guarantees that ensembles in phase space occupy a volume of phase space with remains constant over time; but in dissipative systems, phase space volumes constantly decrease with time. All real engineering systems have some form of dissipation. Sometimes dissipative systems, even those with infinite-dimensional phase space (i.e. partial differential equation models), settle to a low dimensional attractor because of this volume contraction. This is actually a familiar effect: final equilibrium is a point attractor in phase space, a zero-dimensional set; a period limit cycle is a one-dimensional attractor.

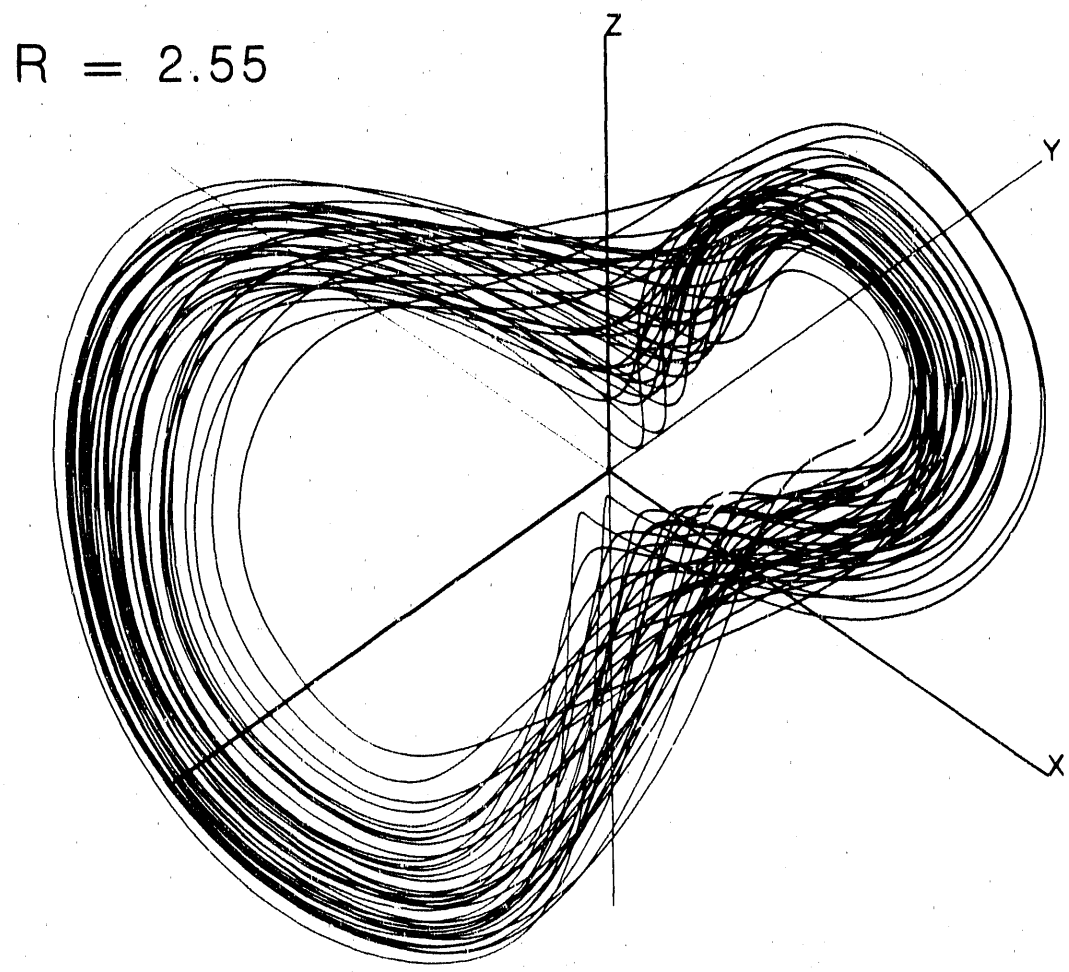

FIGURE 4. Three-dimensional attractor computed from a numerical model of a two-phase flow problem with very high-dimensional phase space.

Large dynamical systems may also settle to small chaotic attractors, which are always more than two-dimensional. A mathematical prescription for finding the dimension of any abstract point set can be applied to chaotic attractors; the resulting number, called the *Hausdorff dimension*, need not be an integer. (Partly for this reason, chaotic attractors are sometimes called strange attractors.) The Hausdorff dimension and other related non-integer dimension numbers for chaotic attractors have been measured and found small in experiments in dynamics of continuous media, such as plasmas[4] and fluids[5], having infinite dimensional phase space.

There are data analysis methods for constructing a phase portrait of a low-dimensional chaotic attractor directly from experimental data, even when the data are only partly complete. If the Hausdorff dimension measured from such a reconstructed orbit is small, then we may hope to visualize the dynamics in a correspondingly low-dimensional subset of phase space. In two notable case studies, geometrically simple chaotic attractors were found in the dynamics of a self-sustained chemical oscillation[6], and in a study of a dripping faucet[7]. In both cases the chaotic attractor was found to be a topological type called the *simply folded band*, originally discovered by Rössler[8] and shown in Figure 5 from two different angles in three-dimensional phase space.

QUALITATIVE GOALS OF NONLINEAR DYNAMIC SIMULATION

The traditional test of good correspondence between approximate and true solutions of initial value problems rests on Hadamard's notion of well-posedness. Typically, one tries to show that uncertainties in the initial data are magnified over a time interval τ by a factor which remains bounded for any given τ. Often one discovers that this uncertainty magnification factor grows as $\exp(\lambda\tau)$, where λ is the largest Lyapunov exponent. Observation and analysis of nonlinear dynamical systems shows it is quite common for λ to be greater than zero, even in the case where long-term steady oscillations (attractors) occur; in fact this property is characteristic of chaotic attractors.

When long term behavior of initial value problems is considered, Hadamard's criterion that solutions should depend continuously on initial conditions becomes too much to ask. Typically nonlinear systems have multiple co-existing attractors; the ensemble of initial states which evolve to a given attractor is the *basin* or catchment region of the attractor. The boundary of each basin is a separator: initial conditions which straddle the boundary end up on different attractors, so the magnification factor can go to infinity because the straddle starts can be moved arbitrarily close to the separator. In other words, the separator is precisely the set where final behavior depends discontinuously on initial conditions. This difficulty is aggravated by the fact that a separator can be tangled, producing a fractal basin boundary [9,10], that is, there can be a thick set of initial conditions where uncertainty magnification is infinite. The reason for this is that in directing our

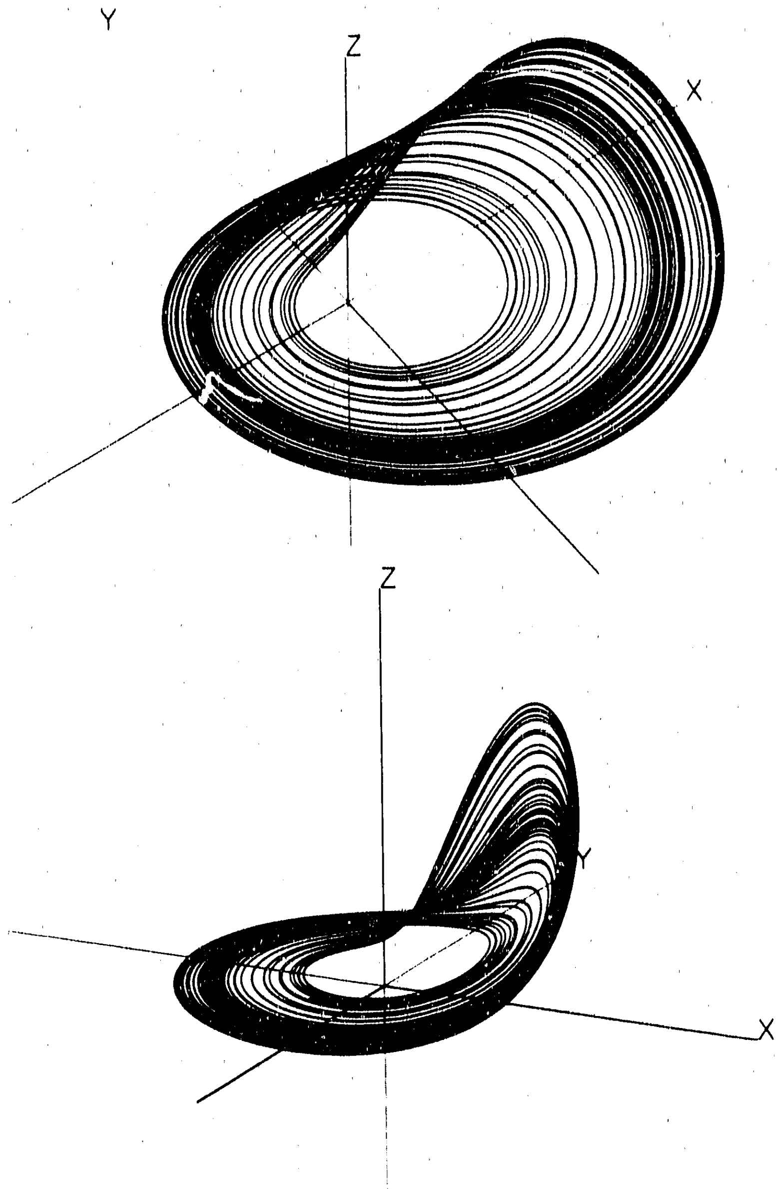

FIGURE 5. Two views of a single post-transient chaos trajectory in Rössler's simply folded band attractor.

attention to long term behavior, we have asked a question about infinity, i.e., about $\tau \to \infty$.

For assessing the performance of any approximation to a dynamical system, specifically, its ability to simulate long-term steady oscillations, it becomes appropriate and indeed essential to begin with qualitative criteria. According to Poincaré, the qualitative criteria should be grounded in the geometry of phase space, and so one must begin with this abstract space in which the orbits of both the true system T and its approximation or model M can be constructed. Even if the orbits of T and of M are known in different and unrelated coordinate systems, comparisons can be made based on topological structure; but it is useful to imagine a single coordinate system applicable to orbits of both T and M.

A common feature of nonlinear dynamical systems is the existence of multiple attractors, i.e. different final behaviors reachable under identical system conditions from different initial states. In simulation of linear dynamics this would be pathological behavior, but in nonlinear dynamics it may well be correct; in fact, it should be expected.

For real systems which include dissipation, the qualitative criteria for comparing the long term behavior of the true system T with its model M are as follows:

(1) Are the attractors of T the same in number as those of M?

(2) Is the location in phase space (locus) of each M attractor roughly the same as the corresponding attractor of T?

(3) Is the dimension (particularly the embedding dimension) of each attractor the same?

(4) Is the topological structure the same?

(5) Is the basin of each M attractor roughly the same as the corresponding basin of T? If the basins are complicated, consider first the largest convex set in each basin; then ask whether tangled boundaries occur in similar regions; finally whether the topological structure of the tangles is the same. Here the geometric theory of *invariant manifolds* [**2**,**3**] in phase space may be helpful, since the boundaries between basins, called *separatrices*, are always invariant manifolds associated with unstable recurrent motions.

Another typical phenomenon in nonlinear dynamics can be observed when a system has one or more parameters called *controls*. In mathematical models these may appear as numbers which are constant for each simulation, but may be changed from one simulation to the next. In real dynamical systems, controls might include throttles, valves, dials, and so on. If both the true system T and its model M are equipped with control parameters, qualitative criteria are formulated in the geometry of control-phase space, which is the Cartesian product of the space of controls

$\{\mu_1, \mu_2, \ldots, \mu_n\}$ with the phase space. Again it is useful to imagine being able to measure these controls in the same way for both T and M, although topological comparisons are possible even if the controls of T and of M are measured in different coordinate systems whose relation to each other is unknown.

Sometimes when a control is evolved very slowly a dissipative dynamical system exhibits a sudden jump in behavior. An example is the sudden collapse of an engineered structure under gradually increasing load. This is caused by the sudden disappearance of an attractor (in this case an equilibrium point) from phase space as the control passes a critical value. It is known that such sudden changes in statics are usefully described by Thom's elementary catastrophe theory[**11**].

Such sudden changes in dynamical behavior, or *bifurcations*, may also affect periodic or chaotic attractors or their basins. As a control parameter such as μ_1 varies, a threshold value may be found across which there is a bifurcation, that is a qualitative change in the structure of the phase portrait, the geometric picture showing attractors, basins, and separators. Some bifurcations – like the intermittency of Pomeau and Manneville[**12**] or the explosion in size of a chaotic attractor first documented by Ueda[**13**] (also called an interior crisis[**14**]) – affect only an attractor. It is also possible for a basin to suddenly change in size – a pure basin bifurcation. The most severe bifurcation type is the blue sky catastrophe or boundary crisis in which an entire attractor suddenly loses stability and disappears from the phase portrait altogether, while at the same time its basin of attraction suddenly becomes part of some contiguous, pre-existing basin (perhaps the basin of the attractor at infinity); see for example[**15**]. For dynamical systems with controls, the qualitative criteria for models are:

(1) What are the loci in control-phase space of the blue sky catastrophes, that is, bifurcations in which an attractor suddenly loses stability and completely disappears from the phase portrait?

(2) What are the loci in control-phase space of the explosions, bifurcations in which the phase space locus of an attractor suddenly explodes in size?

(3) What are the loci of bifurcations where the embedding dimension of an attractor changes suddenly?

(4) If the attractors are low dimensional, is the topological structure of each bifurcation in control-phase space the same for T and M?

(5) What are the loci in control-phase space where basins undergo sudden qualitative changes such as explosions in size or change in topological structure?

The key to topological structure in all these questions was found by Poincaré to be the unstable periodic motions of the dynamical system, and their asymptotic invariant manifolds.

In each of the above series of five criteria, the first criterion should be addressed before proceeding to any further criteria; typically the absence of an expected attractor, or the presence of a spurious one, would be a most serious qualitative flaw in a model or simulation. Depending on the level of accuracy required in a specific application, it may be appropriate to address further qualitative criteria in a series along with quantitative standards of accuracy. Indeed quantitative standards in nonlinear dynamics only make sense in the proper qualitative framework. This can be seen in the geometry of phase space with the aid of correctly designed macroscopic visualization tools.

APPLICATION TO A PROBLEM IN TWO-PHASE FLOW

Let us now turn to an example of how these criteria may be applied in practice. Our example is a numerical simulation using finite difference equations for a two field model of an air/water jet confined in a rectangular box with a small outlet. The two field model is a set of partial differential equations generalizing the Euler equations of fluid motion to two-phase flow by introducing a separate vector field for the motion of each phase, and assuming the phases to be so thoroughly interpenetrating that both vector fields are defined at every point in the flow region (for example by averaging of microscopic fluid velocities).

The basic two-field equations for dynamics of two-phase fluid flow are [**16**]:

$$\partial_t \alpha_i \rho_i + \nabla \cdot \alpha_i \rho_i \vec{u_i} = 0$$

$$\alpha_i \rho_i [\partial_t \vec{u_i} + \vec{u_i} \cdot \nabla \vec{u_i}] + \alpha_i \nabla P = (-1)^i F - f_i$$

for $i = 1$ (air) and $i = 2$ (water), with the constraint $\alpha_1 + \alpha_2 \equiv 1$ relating the phase volume fractions α_i. The interphase momentum transfer is adapted from [**17**]; its components ($\xi = x$ or y) are

$$(F)_\xi = [\mu_\ell / r^2 + \rho_1 |u_{1\xi} - u_{2\xi}| / r] \, (\vec{u_1} - \vec{u_2})_\xi$$

$$r = R\alpha_1\alpha_2$$

depending on a bubble radius R which is presumed constant. There is also dissipation in the form of wall friction f_2 acting on the liquid phase momentum [**18**]. In both of these constitutive relations simple forms were chosen which do not exhibit any discontinuous jump as a function of any argument (such as might occur in constitutive relations whose form depends on flow regime, e.g. bubbly vs. slug flow).

Thus if we observe any very abrupt change in qualitative form of, say, a steady oscillation upon changing slightly the value of a parameter such as R, then we may attribute this to a nonlinear effect in the two-field equations themselves causing a bifurcation. Phase portraits should then be examined for evidence of some specific topological form of bifurcation [**2**,3,19,20].

In spite of the fact that the natural initial value problem for the partial differential equations above is ill-posed, the corresponding finite difference equations can be solved numerically to give well-behaved solutions, given sufficient numerical diffusion in the form of upwind differencing [**21**]. By well-behaved we mean for example that when the interphase drag is made large by setting R small, numerical solutions of the confined jet problem quickly settle to a steady flow with velocity fields $\vec{u_1}$ and $\vec{u_2}$ nearly equal.

Figure 6 shows the finite difference grid used in all simulations. There are 6 unknowns per cell (two scalar fields α_1 and P, plus two vector fields $\vec{u_1}$ and $\vec{u_2}$), so on a 7 x 10 grid the phase space has about 420 dimensions. This number is slightly reduced by boundary conditions including zero normal velocity of both phases at the box walls, a constant pressure of 1.3 bars at the outlet, and constant inlet flow rate of 1.56 kg/sec and quality 0.257% at the inlet.

The numerical model is motivated by experiments with air-water flows reported by Lahey [**22**]. Unfortunately, no data were recorded form these experiments with which to test dynamic simulations. It can only be said that the experiments did show oscillations (in pressure) near the outlet; that the experimental oscillations could often be said to have a dominant frequency of a fraction of 1 Hz; and that hysteresis was very commonly observed while varying flow controls in the experiment.

Lacking the experimental data to assess the numerical simulations of the dynamics against experiment, we can nevertheless use the same qualitative criteria to judge the robustness of the numerical methods. For examples, we select some parameter whose value is subject to doubt, such as a modeling coefficient. In the first series of simulations, the bubble radius R was varied. At each of a number of R values, a simulation was allowed to settle to long term behavior, presumably an attractor. In each case, the initial condition was an attractor for another nearby value of R. Multiple attractors were sometimes found by evolving R in steps toward a specific value from both larger and smaller R values. In this way a partial, schematic control-phase portrait can be constructed, giving qualitative information about sensitivity to the value of R. That is, we may choose two values R_1 and R_2 and apply the criteria above: identify R_1 with T and R_2 with M, and compare phase portraits.

Although it would be difficult in practice to dispose of working control over

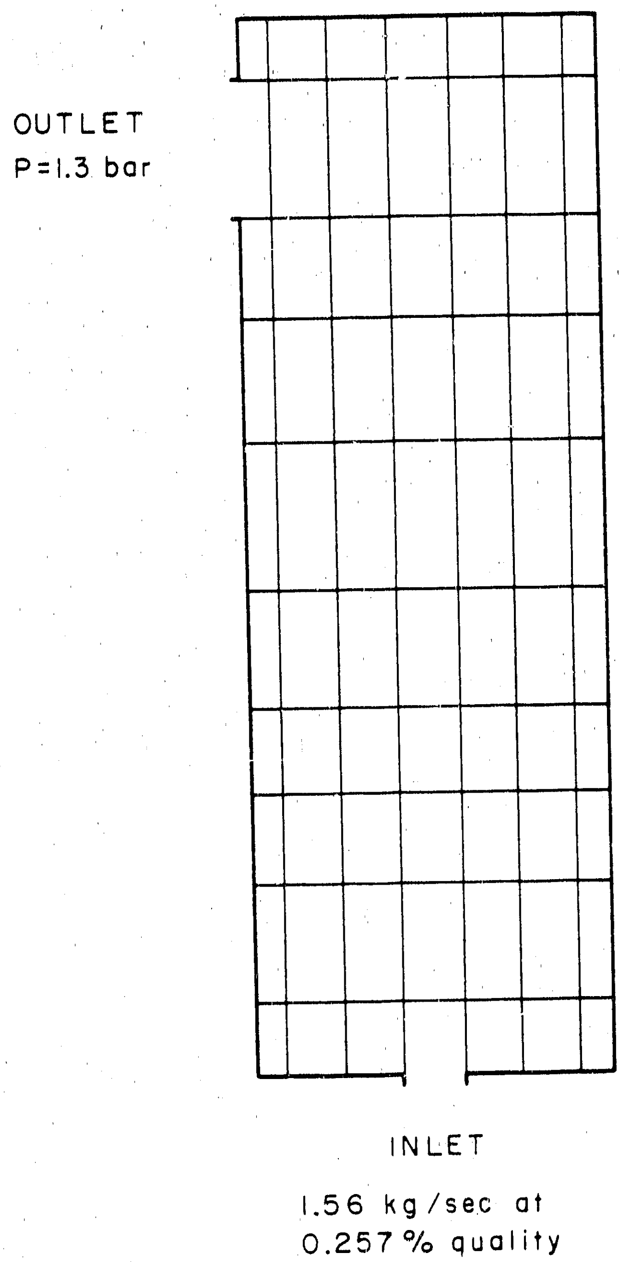

FIGURE 6. Eulerian finite difference grid used for numerical simulations of a confined air/water jet.

bubble radius R in an experiment without changing the boundary conditions, it is nevertheless useful to understand the control-phase portrait with R considered as a control. For example, suppose our model shows a bifurcation near a certain value R^*. By bringing dynamical systems theory to bear, we may be able to confirm that this bifurcation occurs generically on a smooth manifold of codimensional one in multidimensional control space. This means that if we consider another control such as the inlet mass flow rate G_{in} (which could be an independent experimental control), we expect that the same bifurcation observed by varying R at fixed G^* will also be observed by varying G_{in} at fixed R^*. In general we may not know whether to look at $G_{\text{in}} > G^*$ or $G_{\text{in}} < G^*$, but in one of these two directions the smooth bifurcation manifold will undoubtedly be crossed.

On the basis of photographs of the flow it was presumed that plausible values for R might lie in the range from 1mm to 5mm. Over most of this range, simulations settled to long term solutions with long-term oscillation, noticeable for example in fluctuating outlet mass flow rate over a range as wide as 80% to 140% of the steady inflow rate. In at least two narrow regimes of R values, the outlet mass flow rate $G(t) = \alpha_1\rho_1|u_1| + \alpha_2\rho_2|u_2|$ exhibits steady nonperiodic fluctuations. An example was shown in Figure 4 computed with $R = 2.55$ mm. The three-dimensional orbit shown was reconstructed from the time series of G only, using a well-known reconstruction algorithm [**7**,23,24].

Although the projected view of this three-dimensional orbit shows apparent self-crossing, this orbit was also inspected visually using 3d real-time computer graphics, which clearly indicated that there are no self-crossings of the orbit in the three-dimensional reconstructed phase space, and that the orbit can be generated by a smooth vector field in a three-dimensional phase space. Furthermore, it is not difficult to find a plane surface which gives a global Poincaré section, so that the dynamics can be reduced to those of a planar diffeomorphism. Indeed the great coherence of the orbit structure suggests that it may represent a simple chaotic attractor of known qualitative type. Thus it would be possible to apply criteria (2), (3), and (4) above in comparing with other R values to qualitatively assess the robustness of this simulation.

As it happens, however, the criterion (1) is of even greater importance in this case. Figure 7 shows several waveforms for different R values. In all cases except the fourth, $R = 2.6$ mm, initial transients have been completely discarded, and the responses shown represent long term behavior. (A brief transient interval can be seen in the case $R = 2.6$ mm.) The first three cases we obtained by evolving R from 2 mm upward in successive steps, allowing long term behavior to develop at each stage. Any increase of R beyond 2.55 causes a transient to a much larger amplitude oscillation, as shown for $R = 2.6$ and $R = 2.7$ mm. This suggests that the low amplitude attractor experiences a complete loss of stability, that is, a blue sky catastrophe, for R slightly greater than 2.55 mm.

If instead one starts at $R = 2.7$, where the only attractor observed is a high amplitude oscillation, one finds that the value of R may be decreased below 2.55, in fact to 2.4 while still maintaining high amplitude oscillations. That is, in the range $2.4 < R < 2.55$ there are two co-existing attractors, readily distinguished by the amplitude of oscillation; which attractor one observes in a given simulation depends only on the initial conditions. When R is decreased below 2.4, the high amplitude attractor disappears in another blue sky catastrophe.

This situation is summarized in the upper half of Figure 8, where the greatest cyclical maximum of each long-term waveform is shown by a dot; in cases such as $R = 2.4$ where the cyclical maxima are not uniform but cover a range of values, this fact is indicated by a straight line under the corresponding dot. Clearly there is a form of dynamic hysteresis in the range $2.4 < R < 2.55$.

The existence of two such widely disparate waveforms would normally supersede more detailed questions such as the structure of either attractor. We are forced to conclude that these simulations appear to be somewhat robust within the three intervals (2.0, 2.4), (2.4, 2.55), and (2.55, 3); but not across the bifurcation values $R = 2.4$ or $R = 2.55$. By simply checking for the appearance of low or high amplitude oscillations, or both, in the corresponding experiment, one would have strong qualitative grounds for deciding which interval of R values best models reality.

More rigorous assessment of robustness can be made by treating the parameter R as one of two controls. In place of a single phase portrait $P(R_1)$ consider a control phase portrait $P(R)$ for an interval $R_1 < R < R_2$ of control values. Geometrically this portrait is built in a space with the control interval (R_1, R_2) orthogonal to the phase space : the portraits of $P(R)$ are stacked like slices in a loaf of bread. Now pick a second control; we choose w, a parameter in the numerical finite difference approximation scheme. For two values w_1 and w_2, identify the control-phase portrait $P(R, w_1)$ with T and $P(R, w_2)$ with M and use the qualitative criteria for testing control-phase portraits. That is, compare the w_1 loaf of bread with the w_2 loaf.

Such a comparison can be made in crude form by referring to Figure 8, where the lower diagram was computed using $w_2 = 0.7$ corresponding to partial donor cell (upwind) differencing of momentum convection, contrasted with the value $w_1 = 1.0$ (full donor cell differencing) used previously. Note that we are using only a partial representation of the phase portrait (cyclical maxima); in other circumstances, more detailed phase portraits might be needed, but here the two known attractors are

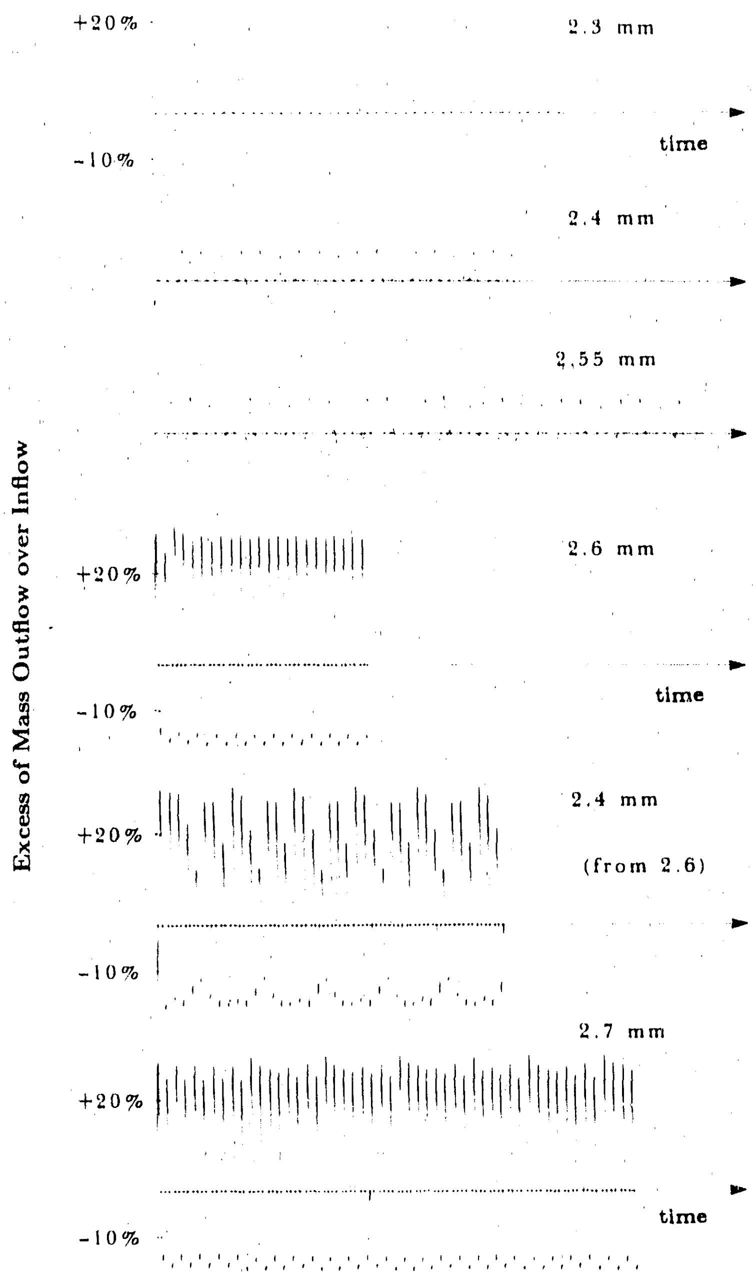

FIGURE 7. Waveforms of outflow versus time in the air/water jet simulations for six different values of the interfacial drag parameter R.

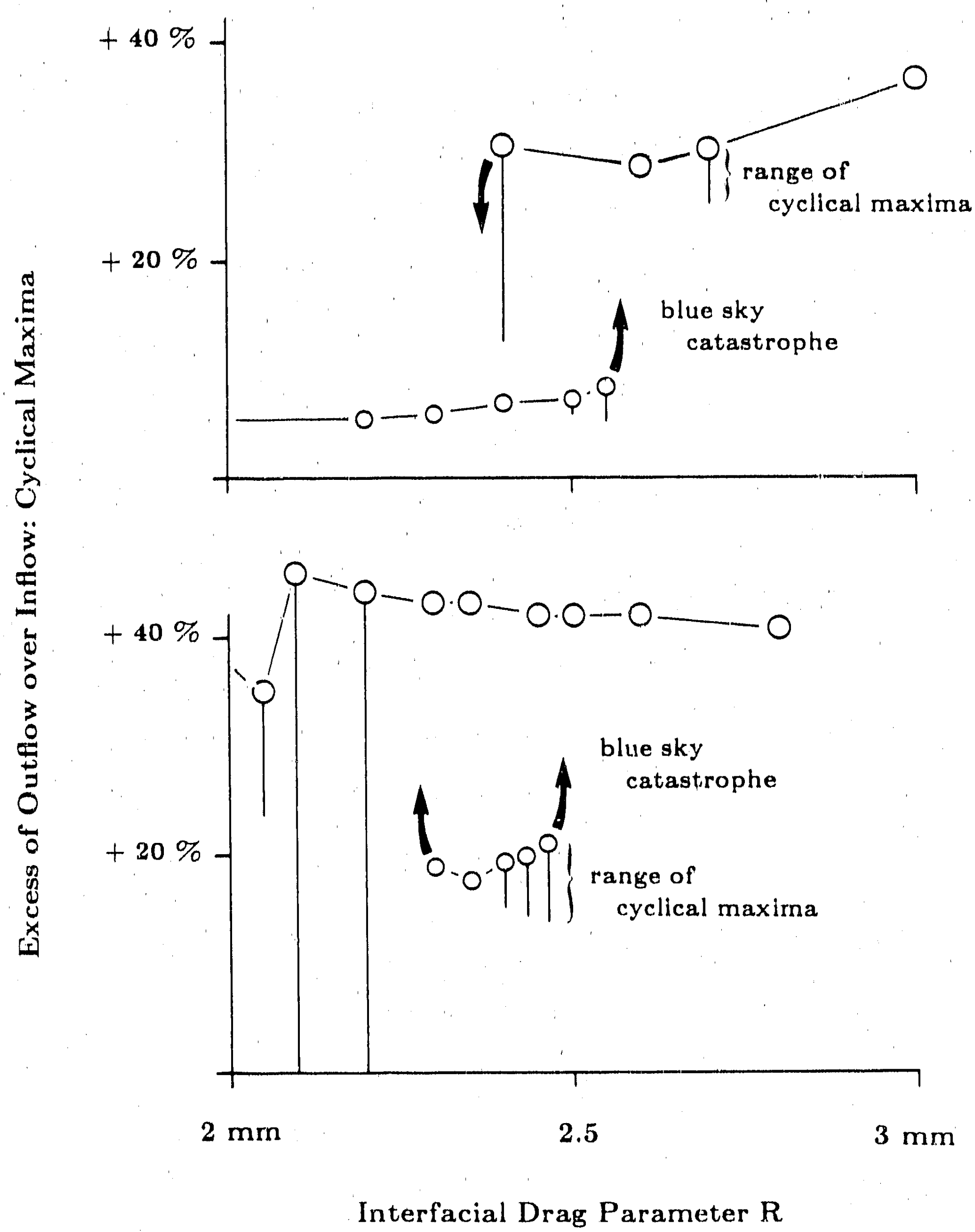

FIGURE 8. Partial control-phase diagrams of the air/water jet simulations in the range $2 < R < 3$, for two different numerical schemes: full donor cell differencing (above) and partial donor cell (below).

readily distinguished by considering only the crudest phase portrait information.

The most striking difference between the two control-phase diagrams in Figure 8 is that in the lower diagram high amplitude oscillations persist over the entire range $2 < R < 3$. There is still a region where high and low amplitude attractors coexist: this is a robust feature of the simulations. The control-phase diagram is also qualitatively robust for R values above the interval of co-existing attractors: upon increasing R, the low amplitude solution loses stability in a blue sky catastrophe, leaving only the high amplitude solution. On the other hand, the diagram to the left of the interval of co-existing attractors is not robust: for $w_2 = 0.7$ the low amplitude oscillation has a blue sky catastrophe as R is decreased, whereas for $w_1 = 1.0$ it was the high amplitude oscillation which lost stability.

Evolving R from $R = 2$ to $R = 3$ and back while holding $w = w_2$ would not yield hysteresis; the low amplitude solution would never be noticed. In fact the low amplitude solutions at $w = w_2$ were found by evolving from the low amplitude solutions at $w = w_1$. This presents additional opportunities for deciding which simulations better represent reality, based on qualitative behavior.

Continuing in this manner, each additional control which is explored systematically adds a further dimension for assessing robustness of the simulations.

ACKNOWLEDGMENT

The author is grateful to Ralph Abraham, Otto Rössler, and Michael Thompson for many stimulating discussions.

REFERENCES

1. Y. Ueda, *Steady Motions Exhibited by Duffing's Equation: A Picture Book of Regular and Chaotic Motions*, in "New Approaches to Nonlinear Problems in Dynamics," P. J. Holmes (ed.), SIAM, Philadelphia, 1980, pp. 311–322.
2. R. H. Abraham and C. D. Shaw, "Dynamics: The Geometry of Behavior, Parts One through Four," Aerial Press, Santa Cruz, California, 1982-89.
3. J. M. T. Thompson and H. B. Stewart, "Nonlinear Dynamics and Chaos," Chichester: John Wiley and Sons, 1986.
4. G. A. Held, C. Jeffries and E. E. Haller, *Observation of chaotic behavior in an electron-hole plasma in Ge*, Phys. Rev. Lett. **52** (1984), 1037–1040.
5. A. Brandstäter, J. Swift, H. L. Swinney, A. Wolf, J. D. Farmer, E. Jen and P. J. Crutchfield, *Low-dimensional chaos in a hydrodynamic system*, Phys. Rev. Lett. **51** (1983), 1442–1445.
6. J.-C. Roux, R. H. Simoyi and H. L. Swinney, *Observation of a strange attractor*, Physica **8D** (1983), 257–266.
7. R. Shaw, "The Dripping Faucet as a Model Chaotic System," Aerial Press, Santa Cruz, California, 1984.
8. O. E. Rössler, *An equation for continuous chaos*, Phys. Lett. **57A** (1976), 379–398.
9. C. Hayashi, Y. Ueda, N. Akamatsu and H. Itakura, *On the behavior of self-oscillatory systems with external forcing*, Electronics and Commun. in Japan **53A** (1970), 31–39.

10. S. W. McDonald, C. Greborgi, E. Ott, and J. A. Yorke, *Fractal basin boundaries*, Physica D **17** (1985), 125–153.
11. J. M. T. Thompson, "Instabilities and Catastrophes in Science and Engineering," John Wiley, Chichester, 1982.
12. Y. Pomeau and P. Manneville, *Intermittent transition to turbulence in dissapative dynamical systems*, Commun. Math. Phys. **74** (1980), 189–197.
13. Y. Ueda, *Explosion of strange attractors exhibited by Duffing's equation*, in "Nonlinear Dynamics," R.H.G. Helleman (ed.), N.Y. Academy of Sciences, New York, 1980, pp. 422–434.
14. C. Grebogi, E. Ott, and J.A. Yorke, *Crises, sudden changes in chaotic attractors, and transient chaos*, Physica D **7** (1983), 181–200.
15. R. H. Abraham and H. B. Stewart, *A Chaotic Blue Sky Catastrophe in Forced Relaxation Oscillations*, Physica **21D** (1986), 394–400.
16. H. B. Stewart and B. Wendroff, *Two-phase flow: models and methods*, J. Comput. Phys. **56** (1984), 363–409.
17. F. H. Harlow and A. A. Amsden, *Numerical calculation of multiphase fluid-flow*, J. Comput. Phys. **17** (1975), 19–52.
18. W. H. Reed and H. B. Stewart, "THERMIT," EPRI Report NP-2032 (1981).
19. R. H. Abraham and J. E. Marsden, "Foundations of Mechanics," 2nd Ed. Reading, Mass.: Benjamin/Cummings, 1978.
20. J. Guckenheimer and P. Holmes, "Nonlinear Oscillations, Dynamical Systems, and Bifurcation of Vector Fields," Springer-Verlag, New York, 1983.
21. H. B. Stewart, *Stability of two-phase flow calculation using two-fluid models*, J. Comput. Phys. **33** (1979), 259–270.
22. R. T. Lahey, Jr., *Two-phase flow phenomena in nuclear reactor technology*, NUREG/CR-0418 (1978); NUREG/CR-1393 (1979).
23. N. H. Packard, J. P. Crutchfield, J. D. Farmer, and R. S. Shaw, *Geometry from a time series*, Phys. Rev. Lett. **45** (1980), 712–716.
24. F. Takens, *Detecting strange attractors in turbulence*, in "Dynamical Systems and Turbulence," D. A. Rand and L. S. Young (eds.), Springer-Verlag, New York, 1980, pp. 366–381.

END

DATE FILMED

11 / 07 / 90